Raman monitoring laser-induced phase transformation in microcrystalline silicon thin films prepared by PECVD

2003 Semicond. Sci. Technol. 18 864

(http://iopscience.iop.org/0268-1242/18/9/309)

INSTITUTE OF PHYSICS PUBLISHING SEMICONDUCTOR SCIENCE AND TECHNOLOGY

Semicond. Sci. Technol. **18** (2003) 864–869 PII: S0268-1242(03)55172-0

Raman monitoring laser-induced phase transformation in microcrystalline silicon thin films prepared by PECVD

S B Concari[1] **and R H Buitrago**[1,2]

[1] Departamento de Física, Facultad de Ingeniería Química (UNL), Stgo. del Estero 2829 (3000), Santa Fe, Argentina
[2] Instituto de Desarrollo Tecnológico para la Industria Química (CONICET-UNL), Güemes 3450 (3000), Santa Fe, Argentina

E-mail: sconcari@fiqus.unl.edu.ar and rbuitre@intec.unl.edu.ar

Received 23 October 2002, in final form 24 June 2003
Published 8 August 2003
Online at stacks.iop.org/SST/18/864

Abstract

The results of a study of phase transformation in hydrogenated microcrystalline silicon thin films prepared from hydrogen-diluted silane and exposed to an Ar^+ laser light are presented. Through Raman spectroscopy, it was determined that the induced phase transformation is interrelated with silane dilution in hydrogen used as a reactive gas in the preparation of the films and, therefore, depends on the grain size and crystalline fraction of the material. Dark conductivity, transmission electronic microscopy (TEM) and atomic-force microscopy (AFM) data have been used to corroborate the Raman measurements. The results show that the sequence of phase transformation in microcrystalline thin films presents different characteristics from those, which are produced in single-crystal silicon structures. The occurrence of a Raman peak at 350 cm^{-1} is attributed to the formation of the Si-XII phase. A thermal model to explain the phase transformation is proposed. To our knowledge, neither the presence of the phase Si-XII nor the phase transformation process in microcrystalline silicon thin films has been reported before.

1. Introduction

There are twelve known phases for silicon. Si-XII is a meta-stable phase that has been first reported by Crain *et al* [1]. It consists of a rhombohedral diamond structure (r8) with eight atoms in the primitive cell. The density of this phase is higher than any of the tetrahedral forms of silicon due to non-bonded neighbour separation in r8, which is substantially shorter than those of the other forms. This reduction in next-near neighbour distance is achieved through important local deviations from tetrahedral bonding, making the r8 phase the most structurally distorted crystalline tetrahedral form of silicon.

As Piltz *et al* [2] have pointed out, the importance of the r8 structure is further increased by the presence of add fold-bonded rings, which are known to greatly affect electronic properties.

The phase-transformation processes induced by compressive stress in bulk silicon have been studied through microindentation [3, 4], microcutting [5, 6] and hydrostatic tests [1, 2]. Such crystallographic studies have established that, for pressures up to 10 GPa, single-crystal silicon structures (c-Si) identified as a phase I (dc) are transformed totally into metallic phase II (β-Sn). As pressure is being slowly reduced to 9.3 GPa, phase XII (r8) starts to form, maintaining itself, down to a pressure of 2.6 GPa. Reducing the pressure even more, phase XII is partially transformed into phase III (bc8), which at pressures smaller than 1.6 GPa transforms to phase I. If the process of depressurization is slow, phases XII, III and I can coexist at normal pressure. Similar studies of phase-transformation processes in silicon thin films have not been reported.

The plasma enhanced chemical vapour deposition technique (PECVD) using hydrogen-diluted silane as a reactant gas is usually employed to deposit hydrogenated microcrystalline silicon (μc-Si:H) thin films. The amount of hydrogen bounded to silicon in the amorphous tissue as well

as in the grain boundaries of the microcrystallites, depends on the dilution grade and both influence the growth rate, the grain size and the residual stress in the films.

Intermediate order in tetrahedrally coordinated silicon thin films has been recently investigated by Tsu *et al* [7], and Sundae-Meya *et al* [8], but in other experiments of crystallization of silicon thin films with laser excimer beam, no phases other than I and amorphous have been detected. In addition, Sundae-Meya *et al* [8] found that higher irradiation power and higher initial hydrogen concentration both lead to films with decreased crystalline size. It is generally accepted that structural disorder of the silicon network is influenced by the hydrogen concentration and the correlations between the hydrogen content and the degree of disorder depend strongly on the preparation method. In addition to the passivation of Si dangling bonds, the hydrogenation induces rearrangement of the Si–Si bonding, so differences in phase transformation are expected for different contents of hydrogen in the films.

Raman spectroscopy is a straightforward and very sensitive method of examining crystalline structures [3, 9, 10] and phase transformations [5, 6] of thin solid films, as well as, a non-destructive way of monitoring stress [3, 5, 11] in those films. However, compressive or tensile stress, grain size, phonon confinement and temperature effects can lead to a misinterpretation of the Raman spectra of these microcrystalline materials [12].

In this paper, we present the results of laser-induced phase-transformation processes of a series of μc-Si:H thin films, prepared under different deposition conditions. Structural characterization of the films was performed through Raman scattering, transmission electronic microscopy (TEM) and atomic-force microscopy (AFM). Dark conductivity (σ_d), as well as, infrared transmission spectra (IR) was measured. A model for hot-spot phase transformation in μc-Si:H thin films is proposed.

2. Experimental details

μc-Si:H thin films were deposited on Corning 7059 glass by PECVD in a capacitive-type radio frequency reactor working at 50 MHz. The 20 cm diameter electrodes were 1.35 cm apart from each other. The reactant gas used was SiH_4, highly diluted in H_2. Silane concentration is defined as

$$C(\mathrm{SiH_4}) = \frac{Q(\mathrm{SiH_4})}{Q(\mathrm{SiH_4}) + Q(\mathrm{H_2})} \qquad (1)$$

with $Q(SiH_4)$ and $Q(H_2)$ being the flow of silane and hydrogen gases, respectively.

We selected a series of undoped samples prepared with a different dilution of hydrogen in the reactant gas to be studied. The applied RF power, the total mixture gas flow, the gas pressure and the substrate temperature were 110 mW cm^{-2}, 40 sccm, 60 Pa and 150 °C, respectively. The nomenclature used to identify the samples is the following: 'DN%' where $N = 2, 3, 4, 5, 6$, according to the value of silane concentration used in the deposition.

To analyse the structure of as-deposited thin films, we collected micro Raman spectra at low power density ($\sim$1 kW cm^{-2}) with a triple Jobin-Yvon T64000 spectrometer equipped with a liquid-N_2-cooled charged coupled device camera. We used the 514.5 nm line of an Ar-ion laser for excitation in a backscattering geometry. A 10X lens provided an apparent spot size of about 10–25 μm. Spectral resolution was 0.5 cm^{-1}.

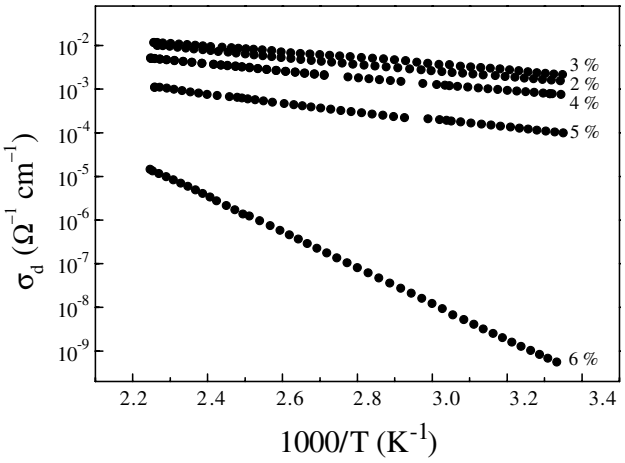

Figure 1. Dark conductivity versus T^{-1} for μc-Si:H films. Silane concentration is shown for each film.

A multichannel Ar laser TRS-600SZ-P with an excitation wavelength of 514.5 nm of a photometric Raman spectrometer was used to induce phase transformation. Power density of the laser beam was $\sim$100 kW cm^{-2}, penetration length $\sim$0.5 μm and the spatial resolution was 1 μm. All spectra were obtained using a 0.5 cm^{-1} step.

σ_d was measured in a standard cryostat at a temperature range of 25 to 150 °C. Surface morphology was studied by means of a Topometric TMX 2000 AFM in air, at normal pressure. Transmission electron diffractograms and micrographs of foils evaporated on grids of Cu were taken at 200 kV in a JEOL JEM 2000FX electron microscope. A 8101M Shimadzu Fourier transformed infrared spectrometer was used to obtain transmission spectra in the range 400–3000 cm^{-1}.

3. Results

All the films studied present an activated dark conductivity as a function of the inverse of temperature [13]. The curves of σ_d versus $T^{-1}$are shown in figure 1. As can be seen, the samples present a clear increase of the dark conductivity from 10^{-9} to 10^{-2} (Ω cm)$^{-1}$ as $C(SiH_4)$ varies from 6% to 2%. The great difference in the σ_d value of samples D6% and D5% shows an onset from amorphous to microcrystalline material.

The results of TEM measurements indicate that μc-Si:H is a heterogeneous mixture of an amorphous matrix and crystallites, growing the crystallites size with hydrogen dilution. Micrograph and its corresponding transmission electron diffractogram of sample D3% are shown in figure 2. The first ring indicates preferential growth in the (111) direction and the small size of the crystallites, which gave rise to the spots in the diffractogram, while the rings correspond to the amorphous matrix. Micrograph show nanocrystals of $\sim$20 nm.

The IR spectra were not well defined due to the thickness of the samples. Peaks at 2100 and 2200 cm^{-1} were not

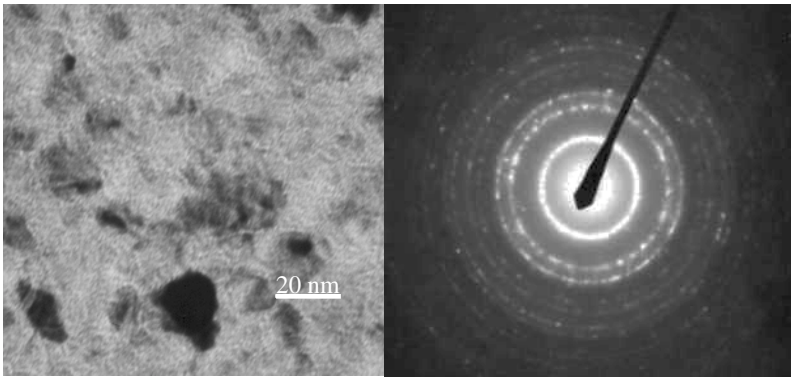

Figure 2. Bright field planar TEM of sample D3% and select area diffraction pattern.

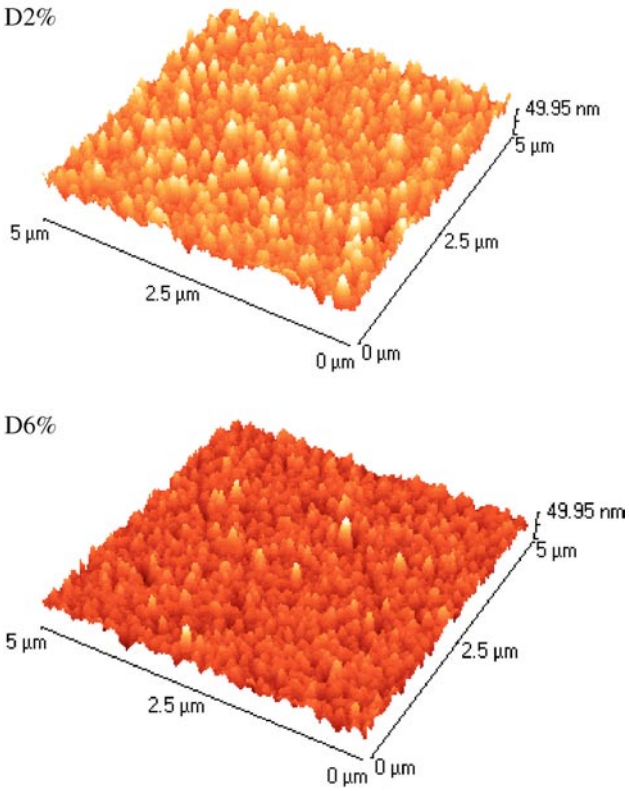

Figure 3. AFM images of D2% and D6% samples.

resolved, and the 650 cm^{-1} peak presents an interference with oxygen signal which was probably adsorbed at the surface. The D6% sample has a higher concentration of hydrogen estimated to 8%. The rest of the samples oscillate around 5%.

The influence of silane dilution in hydrogen on grain size could be studied by AFM. Figure 3 shows the AFM images of the samples D2% and D6%, taken in the same conditions and having the same scales. When the silane is diluted in hydrogen the resulting material has a better defined structure, with increasing coalescence for decreasing silane flow, as can be deduced from the AFM images of the samples D6% and D2%. The bilayer morphology difference may be stated by the value of the root mean square (RMS) roughness: 6.0 nm for D6% and 8.5 nm for D2%. As the thickness of all the samples

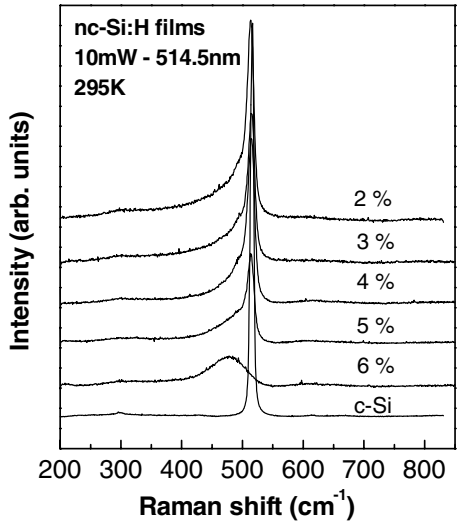

Figure 4. Micro Raman spectra of μc-Si films obtained at $\sim$1 kW cm^{-2} and three successive expositions of 20 s. Spectrum of c-Si is included at the bottom as reference. Silane concentration is shown for each film.

is around 400–650 nm, the difference of the RMS values may be attributed to the difference in the grain size.

Figure 4 shows the micro Raman spectra of the as-deposited films at room temperature. A semi-quantitative measurement of the crystalline volume fraction X_C can be obtained from the deconvolution of the Raman TO phonon band into three components [14]: amorphous, microcrystalline and crystalline. These peaks are fitted with Lorentzian curves centred at $\sim$480 cm^{-1}, 510–514 cm^{-1} and $\sim$520 cm^{-1}, respectively. In order to obtain X_C, the differences in the Raman cross sections should also be taken into account. The following equation is used:

$$X_C = \frac{I_c}{I_c + SI_a} \tag{2}$$

where I_c is the total microcrystalline and crystalline peak area, I_a is the amorphous peak area and S is the relative integrated Raman scattering cross-section for c-Si to a-Si [15].

The calculated crystalline volume fractions of the samples D2%, D5% and D6% were 55%, 35% and 0%, respectively. We have used the data $S = 1$, 13 obtained at 2.4 eV by Tsu *et al* [15]. This result is in agreement with dark conductivity, TEM, IR and AFM data reported above.

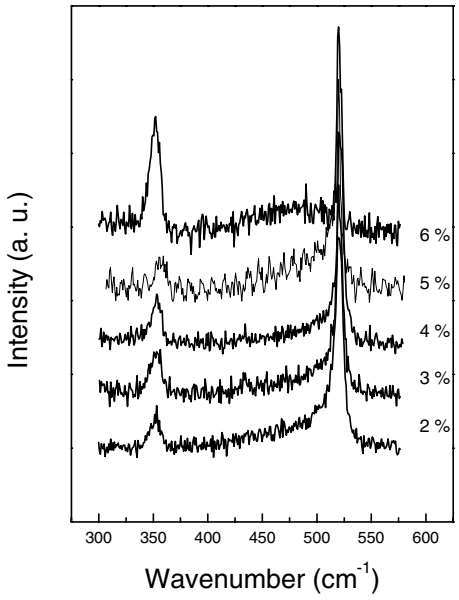

Figure 5. Raman spectra of μc-Si films obtained at $\sim$100 kW cm^{-2} and one scan of 40 s. Spectra are normalized to the peak of 520 cm^{-1}. Silane concentration is shown for each film.

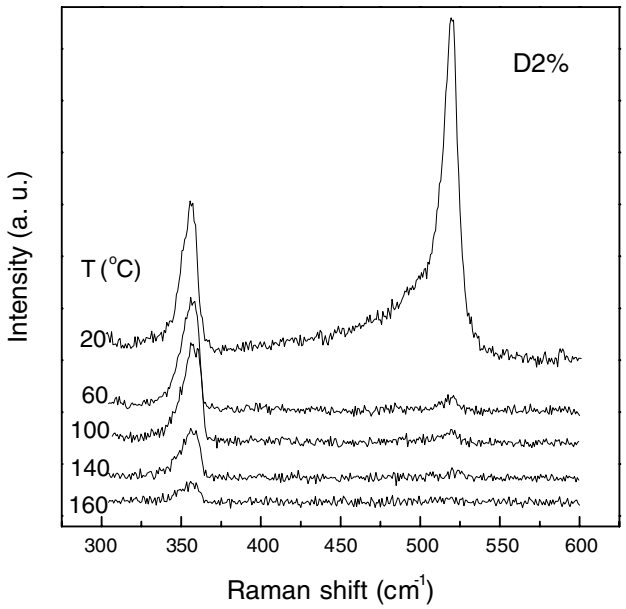

Figure 6. Raman spectra of D2% sample taken at increasing temperatures, which are indicated on each spectrum.

Equation (2) is used by other authors taking S not as the integrated Raman scattering cross-section for c-Si to a-Si, but as a correction to the crystallite size [16, 17]. For the estimated grain size of our samples, volume fraction calculated with both methods differs by 25%.

In figure 4 it can also be appreciated that, while the concentration of silane in the mixture of reactive gases decreases, the peak at 520 cm^{-1} (phase Si-I) grows. The broad one at 480 cm^{-1}, due to the amorphous phase, shifts to higher frequency and decreases until disappearing at high hydrogen dilution.

The peak position of TO Raman signal is 520 cm^{-1} for single crystalline but it shifts to lower frequencies (510–514 cm^{-1}) as microcrystalline grain size decreases [7]. We do not think as other authors do that this peak can be attributed to a phonon contribution of the intergranular surface [18], a phonon confinement effect [19], nor the presence of the crystalline phase Si-IV [4, 5, 11]. We believe that it can be attributed to a non-homogeneous dispersion of grains [5, 7, 20]. This point will be discussed below.

Exposing the films to the Raman laser beam of a power superior to 40 mW modified the Raman spectra showing an extra peak identified as the crystalline phase Si-XII (r8) with a principal TO peak at 350–353 cm^{-1} [2, 4, 5]. In figure 5, we can observe the corresponding Raman spectra of the films exposed for 40 s. The presence of phase III (bc8) is not detected as there is no differentiated peak at $\sim$430 cm^{-1} in the dispersion Raman spectrum.

Using 6% of diluted silane we deposited films of variable thickness from 10 to 60 nm on 7059 Corning glass and on stainless steel. On the film deposited on glass, two peaks were registered at $\sim$520 cm^{-1} and $\sim$353 cm^{-1}. This took place even on the films with the minimum thickness after exposing for 40 s at a laser power of 40 W. On the other hand, on stainless steel, a thickness of more than 40 nm was required in order to observe the crystalline phases on a dominant amorphous base.

The absence of a 430 cm^{-1} peak and other peaks indicates that μc-Si:H phase transformation presents different characteristics from those which are produced in the single crystalline silicon, as has been reported in mechanical tests at room temperature [1–4, 6]. These differences could lie in the fact that the temperature of the sample in this study is much higher than room temperature. For the power and diameter of the laser used, the mean temperature could be approximately 260 °C [3], but it could even reach $\sim$700 °C at the centre spot [12].

In situ Raman spectra of the samples were taken at different increasing temperature from 20 °C to 500 °C. In figure 6 results for D2% are shown. In all the spectra, only the two peaks at 520 cm^{-1} and 353 cm^{-1}were observed. As expected, due to greater phonon dispersion, the intensity of both peaks decreased as the temperature was increased. The peak at 520 cm^{-1} being more sensitive disappeared at 160 °C. This experiment proves that the peak at 353 cm^{-1} corresponds to a quite stable crystalline phase at high temperature.

Another interesting fact to note in figure 6 is that the peak position of phases I and XII remains in the same position, within the experimental error. However, increasing temperature should make the TO Raman peak shift towards lower frequencies [12, 21]. This can be explained as follows: as has been well established for both crystalline and amorphous silicon that the increase of the compressive stress makes the TO peak shift to higher frequencies [22, 23], the effects of temperature could then be compensated with the effects of the compressive stress over the sample volume in our films.

Select area electron diffraction showed the presence of sharp spots, including (111), (220) and (311) reflections (figure 2). The presence of the last two spots clearly indicated that the microcrystallites had the long-range order needed to establish such crystalline diffraction. As Tsu *et al* [7] state, rather than offering evidence of intermediate order, such as phase Si-IV, the 510–514 cm^{-1} Raman scattering can be

considered due to the microcrystallites, where small particle effects lead to observing more of the phonon spectrum, thus causing the apparent shift to lower frequencies as shown by Richter *et al* [19].

From figure 6 we can observe that the relative amount of phase Si-XII decreases with hydrogen dilution. As hydrogen bonded in any way to Si atoms is believed to contribute to the relief of stress in the samples [24], and the presence of phase Si-XII in stressed material, there may be other reasons, which provoke the films with high crystal fraction to have higher thermal conductivity and lower residual stress than those films with low crystal fraction, that contain amorphous phase, than higher hydrogen concentration.

The differences in phase Si-XII growth in the films deposited on glass and stainless steel can also be explained in terms of a thermal effect. Thermal conductivity and dissipation of stainless steel are greater than those of glass. Therefore, the temperature of the sampling volume and compression tensions of films deposited on stainless steel would be smaller than those deposited on glass.

On the other hand, the sampling volume at a high temperature could present a different pattern of structure phase transformation than at room temperature. The Si-XII phase, which is more stable and may require less compression, would prevail over the Si-III phase. However, at present, there are factors that are not known about these transformations. Gupta and Ruoff [25] have shown that for single crystals in the (111) direction, semiconducting–metallic transition is activated at a lower compressive stress than along the (100) direction on single crystals. Glacing x-ray diffraction provided very low-resolution spectra, which showed a preferential growth in the (111) direction of our microcrystalline films. As a result, no presence of phase III could be explained by this fact.

In figure 6 it can be observed that the height of the peak at 353 cm^{-1} decreases with dilution of silane. This fact reveals that the relative amount of the Si-XII phase is smaller for the sample D2%, corresponding to the greater crystalline fraction and presumably larger grain size. As the presence of the Si-XII phase is assigned to compression tensions in the films, we can conclude that residual tensions in the μc-Si decrease with crystal fraction.

Differences of the phase transformation for samples D2% to D6% may be due to this effect.

The presence of crystalline phase Si-XII in μc-Si:H films could be explained as a structure transformation originating in a small volume corresponding to the zone exposed to the laser beam. As the spot is at a higher temperature than the rest of the film due to its low thermal conductivity, the sampling volume is compressed by the cooler surrounding material, thus inducing a higher compression state. As exposition time increases, local temperature also rises. So we can assume higher compression given an increase of the intensity of the phase Si-XII peak related to the phase I peak.

When phases amorphous and Si-I are both present, an important aspect, not clear from the spectra, is which of them transforms to Si-XII. Measurements accomplished on totally amorphous material show that both Si-I and Si-XII phases grow simultaneously. So, the crystallization induced by the laser beam in microcrystalline silicon films is summarized in the transformation of the amorphous phase into phase I and then by compression tensions, to phase Si-XII. Reinterpretation of the asymmetry of the peak at 520 cm^{-1}, may be done in terms of a non-homogeneous distribution of grain size, instead of the presence of phase Si-IV. Also, in the sample studied, Kobiiska and Solin [26] have found no evidence of a transformation from Si-III to this wurzite phase caused by sample heating in the focused laser. They did observe however, a weak line at 355 cm^{-1}. At that time they were not able to identify it with any known Si phase.

4. Conclusions

All the characterization methods used, point out that the series under study is microcrystalline with different degrees of volume crystal fraction. IR, AFM, TEM, conductivity and x-ray results are all consistent with the micro Raman spectra. Increasing the Raman laser power produces a change in the film structure. Si-I, as well as a-Si, transforms to an intermediate phase Si-XII.

From what has been reported here, we can conclude that crystalline phase Si-III, present in single crystals under compression tensions at room temperature and in equilibrium with phase Si-XII and Si-I, is not detected in the μc-Si thin films. In the same way, other effects overlap peak shift from 520 cm^{-1} towards 510 cm^{-1}, but we do not think it is due to the presence of phase Si-IV. TO Raman peak can be found at lower frequencies than 520 cm^{-1}(even as low as 508 cm^{-1}) due to small particle effects [7].

Therefore, we propose a model of phase-transformation process for the silicon in the form of amorphous or microcrystalline thin films as the following: the amorphous phase crystallizes directly in Si-I phase by the effect of the temperature. This one arrives at phase Si-XII without going through phase Si-III due to the effect of high temperature and compression stress in the films.

The Si-XII phase is presented with other phases in a single-crystal silicon submitted to pressures in the range 1.6–2.6 GPa [2]. The residual tensions in the amorphous silicon, always present surrounding the microcrystals and measured by different methods [27–29] are in the range 0.7–1.0 GPa. The occurrence of a Raman peak at 350 cm^{-1}, attributed to the Si-XII phase, suggests that the focalized high power laser beam should increase the residual tensions of the thin films to values higher than 1.6 GPa.

Acknowledgments

This work has been supported by CONICET (PID No 4808/96) and by the Universidad Nacional del Litoral (project CAI+D 96–97 E-014). The authors would like to thank Dr Alejandro Fainstein for the micro Raman spectra and Dr María Teresa Gutierrez for the TEM and AFM measurements.

References

[1] Crain J, Ackland G J, Maclean J R, Piltz R O, Hatton P D and Pawley G S 1994 *Phys. Rev.* B **50** 13043
[2] Piltz R O, Maclean J R, Clark S J, Ackland G J, Hatton P D and Crain J 1995 *Phys. Rev.* B **52** 4072
[3] Lucazeau G and Abello L 1997 *J. Mater. Res.* **12** 2262
[4] Kailer A, Gogotsi Y G and Nickel K G 1997 *J. Appl. Phys.* **81** 3057

[5] Gogotsi Y, Baek C and Kirscht F 1999 *Semicond. Sci. Technol.* **14** 936
Gogotsi Y, Baek C and Kirscht F 1999 *Semicond. Sci. Technol.* **14** 1019 (erratum)
[6] Tanikella B V, Somasekhar A H, Sowers A T, Nemanich R J and Scattergood R O 1996 *Appl. Phys. Lett.* **69** 2870
[7] Tsu D V, Chao B S and Jones S J 2003 *Sol. Energy Mater. Sol. Cells* **78** 115–41
[8] Sundae-Meya A, Gracin D, Dutta J, Vlahovic B and Nemanich R J 2001 *Mat. Res. Soc. Symp. Proc.* **664** 691
[9] Campbell I H and Fauchet P M 1986 *Solid State Commun.* **58** 739
[10] Lengsfeld P, Nickel N H and Fuhs W 2000 *Appl. Phys. Lett.* **76** 1680
[11] Paillard P, Puech P and Sirvin R 2001 *J. Appl. Phys.* **90** 3276
[12] Viera G, Huet S and Boufendi L 2001 *J. Appl. Phys.* **90** 4175
[13] Concari S B and Buitrago R H 2003 *J. Appl. Phys.* **94** at press
[14] Kamei T, Stradius P and Matsuda A 1999 *Appl. Phys. Lett.* **74** 1707
[15] Tsu R, González-Hernández J, Chao S S, Lee S C and Tanaka K 1982 *Appl. Phys. Lett.* **40** 534
[16] Schropp R E I and Zeman M 1998 Amorphous and microcrystalline silicon solar cells *Modelling, Materials and Device Technology* (UK: Kluwer) 49
[17] Bustarret E, Hichicha H A and Bunei M 1988 *Appl. Phys. Lett.* **52** 1675
[18] Kalkan A K and Fonash S 1997 *Mat. Res. Soc. Symp. Proc.* **467** 319
[19] Richter H, Wang Z P and Ley L 1981 *Solid State Commun.* **39** 625
[20] Veprek S, Sarrot F A and Iqbal Z 1987 *Phys. Rev.* B **36** 3344
[21] Cerqueira M F and Ferreira J A 1999 *J. Mater. Process. Tech.* **92–3** 235
[22] Hishikawa Y J 1987 *Appl. Phys.* **62** 3150
[23] Danesh P, Savatinova I, Toneva A and Liarokapis E 1996 *J. Non-Cryst. Solids* **204** 265
[24] Street R A 1991 *Hydrogenated Amorphous Silicon* (Cambridge: Cambridge University Press)
[25] Gupta M C and Ruoff A I 1980 *J. Appl. Phys.* **51** 1072
[26] Kobiiska R J and Solin S A 1972 *Phys. Rev. Lett.* **29** 725
[27] de Lima M M, Lacerda R G, Vilcarromero J and Marques F C 1999 *J. Appl. Phys.* **86** 4936
[28] Spanakis E, Stratakis E, Tzanetakis P, Fritzsche H, Guha S and Yang J 2001 *ICAMS* 19
[29] Danesh P, Pantchev B, Grambole D and Schmidt B 2001 *J. Appl. Phys.* **90** 3065